

# ELECTROLUMINESCENCE OF METAMORPHIC $\text{In}_x\text{Al}_{1-x}\text{As} / \text{In}_x\text{Ga}_{1-x}\text{As}$ HEMTs ON GaAs SUBSTRATE

N. Cavassilas\*, F. Aniel\*, A. Nojeh\*, R. Adde\*,

M. Zaknoue\*\*, S. Bollaert\*\*, Y. Cordier\*\*, D Théron\*\*, and A Cappy\*\*

\*Institut d'Electronique Fondamentale, U.M.R.- C.N.R.S 8622  
Université Paris XI, 91405 Orsay Cedex, France.  
[nicolas.cavassilas@ief.u-psud.fr](mailto:nicolas.cavassilas@ief.u-psud.fr)

\*\*Institut d'Electronique et de Microélectronique du Nord, U.M.R.- C.N.R.S 8520  
Avenue Poincaré, Université de Lille I, BP 69, 59652 Villeneuve d'Ascq Cedex, France.  
[zaknoue@iemnserv.iemn.univ-lille1.fr](mailto:zaknoue@iemnserv.iemn.univ-lille1.fr)

## ABSTRACT

*We present the first impact ionization investigation by electroluminescence of  $\text{In}_x\text{Al}_{1-x}\text{As} / \text{In}_x\text{Ga}_{1-x}\text{As}$  metamorphic High Electron Mobility transistors on GaAs. Two Indium content are investigated. First we observe the decrease of the detrimental effect of impact ionization with the decrease of the Indium content. Second, the electroluminescence measurements illuminate the functional relationship between impact ionization and the kink effect. In these metamorphic HEMT's, we suggest that both kink effect and impact ionization threshold are originated to detrapping process of deep levels in the large band gap layer.*

## INTRODUCTION

Impact ionization, which induces the generation of electron-hole pairs by avalanche multiplication due to hot carriers in high electric field regions of semiconductors, is a well-known process in field-effect transistors. It limits the maximum operating voltage of these transistors. The phenomenon is all the more detrimental in channel lattice-matched (LM) HEMT's on InP since the energy threshold required for ionization is low due to the small band gap of  $\text{In}_{0.53}\text{Ga}_{0.47}\text{As}$ , Bud and Hess (1). At the same time, studies of InP-based HEMT's have shown the superiority of these structures in microwave applications over GaAs-based transistors.

Several solutions have been proposed to reduce impact ionization effects in InGaAs channel HEMT's. One of the best is the lattice matched composite channel InP-based HEMT, Maher et al (2) and Cavassilas et al (3). However the microwave performances of these devices are not as good as those of single channel HEMTs, Maher et al (2), and require an InP substrate.

The metamorphic (MM) HEMT using an unstrained  $\text{In}_x\text{Al}_{1-x}\text{As} / \text{In}_x\text{Ga}_{1-x}\text{As}$  heterostructure grown on GaAs, Zaknoue et al (4), Bollaert et al (5), is an alternative solution. The main benefit of MM-HEMT is to use a GaAs substrate, which is less expensive and less breakable than InP, while keeping microwave performances comparable to LM-HEMT's on InP. Also, the ionization coefficient depends on the indium content  $x$  in the  $\text{In}_x\text{Ga}_{1-x}\text{As}$  channel. Consequently, a study of impact ionization in MM-HEMT's with different indium contents is an important issue.

Our main investigation tool of impact ionization in HEMT's is electroluminescence spectroscopy (EL). Electrons and holes created by impact ionization can recombine

radiatively, giving rise to electroluminescence. EL spectroscopy constitutes an efficient approach to probe both the localization and the energy distribution of carriers versus bias conditions, Cavassilas et al (3), and Sylvestre et al (6).

In this paper, we present an experimental investigation of impact ionization at room temperature by electroluminescence in ultra-short gate ( $L_G = 0.1$  and  $0.15 \mu\text{m}$ ) MM-HEMTs with two different indium contents ( $x = 0.35$  and  $0.5$ ). Our study relies on EL spectroscopy correlated with electrical characterization.

## SAMPLE AND EXPERIMENTAL SETUP

Metamorphic InAlAs/InGaAs heterostructures have been grown by Molecular Beam Epitaxy. The multilayer structure is given in Fig. 2. The inverse step graded buffer of InAlAs is used to accommodate the lattice mismatch parameter between the active layers and the substrate. The  $\bullet$ -doping content is  $10^{13} \text{ cm}^{-2}$  for  $x = 0.35$  and  $5.5 \times 10^{12} \text{ cm}^{-2}$  for  $x = 0.5$ . The MM-HEMT's have a T-shaped gate ( $0.1 \times 100 \bullet \text{ m}^2$  and  $0.15 \times 100 \bullet \text{ m}^2$ ) with a total recess length of  $0.4 \bullet \text{ m}$ , Zaknune et al (4). The thickness of the doped cap layer ( $6 \times 10^{18} \text{ cm}^{-3}$ ) is  $120 \text{ \AA}$  for  $x = 0.35$  and  $100 \text{ \AA}$  for  $x = 0.5$ . The breakdown voltage is  $3 \text{ V}$  for  $0.5 \text{ MM-HEMT's}$  and  $4 \text{ V}$  for  $0.3 \text{ MM-HEMT's}$ .

In this EL study at  $300 \text{ K}$ , the device is mounted on a standard coplanar probe station. The  $50 \bullet$  impedance at the probe tips improves considerably the bias rang of stable operation of the HEMT's. A focusing optics collects the emitted light by the device on the entrance slit of a  $0.64 \text{ m}$  monochromator and detected with a liquid nitrogen cooled germanium detector. The experimental setup is given by Aniel et al (7).

## RESULTS AND DISCUSSIONS

The Fig. 2 shows typical EL spectra measured versus energy, in bias conditions corresponding to the maximum of EL intensity. Because of the breakdown voltage, the drain voltage is limited to  $2 \text{ V}$  for  $x = 0.5$  and  $3 \text{ V}$  for  $x = 0.35$ . The  $V_{GS}$  value which gives the maximum EL intensity is approximately  $V_{GS} = -0.4 \text{ V}$  for both transistors. A main peak centered near  $0.8 \text{ eV}$  for  $x = 0.5$  and  $0.94 \text{ eV}$  for  $x = 0.35$  is observed. These peaks can be attributed to direct recombination in the InGaAs channel (quantum well), of electrons in the first conduction sub-band E1 and of holes in the valence HH1 sub-band. This assignment is confirmed by the calculation of the  $\text{In}_x\text{Ga}_{1-x}\text{As}$  band gap at  $300 \text{ K}$  ( $0.78 \text{ eV}$  for  $x = 0.5$  and  $0.93 \text{ eV}$  for  $x = 0.35$ ). One also observes, at  $x = 0.35$ , the recombination between the second conduction sub-band E2 and the valence sub-band HH1 at  $1.05 \text{ eV}$ , which is clearly visible as a shoulder (Fig. 2). This recombination is not observed for  $x = 0.5$  which remains to be explained.

From the high energy tail of the EL spectra an equivalent carrier temperature  $T_c$  is extrapolated, Gaddi et al (8). The  $T_c$  values are  $1000 \text{ K}$  for  $x = 0.5$  and  $1500 \text{ K}$  for  $x = 0.35$ . We can conclude from the small value of these temperatures that the radiative recombination in the InGaAs channel is mainly located in the source-gate access for both transistors as previously observed in LM HEMT's on InP, Shigekawa et al (9).

Table 1 gives the measured electroluminescence threshold  $V_{TH}$  for different gate lengths and the value  $V_{EL-T}$  corrected for the voltage drop in the device source and drain access resistances. The latter have been calculated using de embedded HF measurements of the cold bias FET and analytical extraction, as in Dambrine et al (10). The measured  $V_{TH}$  and  $V_{EL-T}$  are smaller for  $x = 0.5$  than for  $x = 0.35$  in agreement with the lower band gap energy of  $\text{In}_{0.5}\text{Ga}_{0.5}\text{As}$ . One can conclude that impact ionization is less detrimental in the  $0.35 \text{ MM-}$

HEMT, even if carrier heating can be higher as illustrated by the  $T_c$  determination and the EL intensity (Fig. 2).

The gate length has an influence on  $V_{EL-T}$ . For  $L_G = 0.1 \mu\text{m}$   $V_{EL-T}$  is smaller than for  $0.15 \mu\text{m}$  showing the enhancement of carrier heating in the shorter gate-length HEMTs. For such short gate lengths carrier heating occurs under the gate as compared with longer gate length HEMT's where impact ionization takes place in the gate drain access. As the gate length becomes smaller the rate of ballistic carriers increases and the impact ionization threshold voltage decreases towards a limit very close to the material band gap when the voltage drop due to access resistances is taken into account. Impact ionization is almost due to the distribution tails of very hot carriers which is mainly depending on the carrier concentration and the local electrical field intensity. At shorter gate length the mean free path of optical phonon scattering becomes larger as compared with the gate length.

We point out the small values of  $V_{EL-T}$  at  $x=0.5$  particularly for  $L_G = 0.1 \mu\text{m}$  which is smaller than  $1.1x E_G(\text{InGaAs})$ , an accepted value for energy threshold of impact ionization (Table. 1). When observing the corresponding I-V characteristics in Fig. 3, one can underline the correlation between the kink of the drain current slope in the saturation regime and the threshold of luminescence. The kink effect is observed only for  $x = 0.5$  and is more visible in the  $0.1 \mu\text{m}$  gate length device. This last point illustrates the correlation between kink effect and low impact ionization threshold in the  $0.5 \text{ MM-HEMT}$ 's.

Our interpretation of the luminescence observed below the band gap energy is that hot electrons in the quantum well are not provided solely by the source access but can originate from the InAlAs layer below the gate. The kinetic energy of such carriers crossing the heterojunction from the large band gap InAlAs to the small band gap InGaAs channel is increased by the conduction band discontinuity energy ( $\Delta E_C = 0.51 \text{ eV}$  for  $x = 0.5$ , Chen et al (11)). If the electron transfer occurs under the gate it may reach easily the impact ionization energy threshold.

The reduction of the kink in the I-V characteristics under illumination, observed in Fig. 3, reveals that traps play a prominent role on the device electrical behavior. The difference between illuminated and dark I-V characteristics recorded respectively at constant  $V_{GS}$  and at constant  $V_{DS}$  (not shown) suggests that deep levels are located in the layers above the quantum well. The traps in the  $\text{Al}_{0.5}\text{In}_{0.5}\text{As}$  of our MM-HEMT's behave similarly as in  $\text{Al}_{0.48}\text{In}_{0.52}\text{As}$  which has been intensively studied.

Electrons trapped in the AlInAs layers can be detrapped by a field assisted emission mechanism (Poole-Frenkel) and transfer in the quantum well. This is consistent with the kink observed in the I-V characteristics. The full mechanism is very "efficient" because the detrapped carriers after spatial transfer can create two carriers (an electron and a hole by impact ionization) in the undoped quantum well where carrier velocity is larger. Therefore if  $N_{DT}$  is the concentration of detrapped carriers from deep levels, it results an increase of the carrier concentration of  $3N_{DT}$  in the source-drain current.

In conclusion, in the case of the  $0.5 \text{ MM-HEMT}$ 's, we have been able to show the correlation between the kink and the ionization as in Somerville et al (12), and the correlation between the kink and trapping effect as in Georgescu et al (13).

Concerning the  $0.35 \text{ MM-HEMT}$ 's, there are also trapping centers as light influences the electrical characteristics. However there is no kink effect (not shown). Moreover the ionization thresholds are larger than the channel gap energy (Table. 1). Therefore, for  $x = 0.35$  the trapping centers in AlInAs could have a different nature.

## CONCLUSION

We have presented the first experimental investigation of impact ionization in MM-HEMTs for different Indium contents by electroluminescence. We have shown the shift of luminescence peak and of the EL threshold with values Indium content. Also, drain voltage variation of the EL threshold compared with the band gap energy values show the correlation between impact ionization threshold and kink effect observed in 0.5 MM-HEMT's. These phenomena are related to electron detrapping from deep levels in the wide band gap InAlAs layer. The two phenomena are not clearly observed in 0.35 MM-HEMT's. It is possible that trapping centers in  $\text{Al}_{0.65}\text{In}_{0.35}\text{As}$  have a different nature.

## REFERENCES

- 1 J. Bude, and K. Hess, "Threshold of impact ionization in semiconductors," 1992, J. Appl. Phys., vol. 72, pp. 3554-3561.
- 2 H. Maher, J. Décobert, A. Falcou, M. Le Pallec, G. Post, Y. I. Nissim, and A. Scavennec, "A triple channel HEMT on InP (Camel HEMT) for large-signal high-speed applications," 1999, IEEE Trans. Electron. Device., vol. 46, pp. 32-37.
- 3 N. Cavassilas, F. Aniel, P. Boucaud, R. Adde, H. Maher, J. Décobert, and A. Scavennec, "Electroluminescence of composite channel InAlAs/InGaAs/InP/InAlAs high electron mobility transistor," 2000, J. Appl. Phys., vol. 87, pp. 2548-2552.
- 4 M. Zaknoune, B. Bonte, C. Gaquière, Y. Cordier, Y. Druelle, D. Théron and Y. Crosnier, "InAlAs/InGaAs Metamorphic HEMT with high current density and high breakdown voltage," 1998, IEEE Electron. Device. Lett., vol. 19, pp. 345-347.
- 5 S. Bollaert, Y. Cordier, H. Happy, M. Zaknoune, V. Hoel, S. Lepilliet, and A. Cappy, "Metamorphic  $\text{In}_x\text{Al}_{1-x}\text{As}/\text{In}_x\text{Ga}_{1-x}\text{As}$  HEMTs on GaAs Substrate : The Influence of In Composition," 1998, IEDM, San Francisco , USA.
- 6 A. Sylvestre, F. Aniel, P. Boucaud, F.H. Julien, P. Crozat, A. De Lustrac, R. Adde, Y. Jin, and J. P. Praseuth, "Low temperature electroluminescence spectroscopy of high electron mobility transistor on InP," 1996, J. Appl. Phys., vol. 80, pp. 464-469.
- 7 F. Aniel, P. Boucaud, A. Sylvestre, P. Crozat, F.H. Julien, R. Adde, and Y. Jin, "Electroluminescence spectroscopy of AlGaAs/InGaAs and AlGaAs/GaAs high-electron-mobility transistors," 1995, J. Appl. Phys., vol. 77, pp. 2184-2189.
- 8 R. Gaddi, G. Meneghesso, M. Pavesi, M. Peroni, C. Canali, and E. Zanoni, "Electroluminescence analysis of HFET's Breakdown," 1999, IEEE Electron. Device. Lett., vol. 20, pp. 372-374.
- 9 N. Shigekawa, T. Enoki, T. Furuta and H. Ito, "Electroluminescence of InAlAs/InGaAs HEMTs lattice-matched to InP substrates," 1995, IEEE Electron. Device. Lett., vol. 16, pp. 515-517.
- 10 G. Dambrine, A. Cappy, F. Heliodore and E. Playez, "A new method for determining the FET small-signal equivalent circuit," 1988, IEEE Trans. Microwave. Theory. Tech., vol. 36, pp. 1151-1159.
- 11 J. Chen, JM. Fernandez, and HH. Wieder, "Composition dependent transport properties of strain relaxed  $\text{In}_x\text{Ga}_{1-x}\text{As}$  ( $x < 0.45$ ) epilayers," 1992, App. Phys. Lett., vol. 61, pp.1116.
- 12 M H. Somerville, J. A. Alamo, and W. Hoke, "Direct Correlation Between impact ionization and the kink effect in InAlAs/InGaAs HEMT's," 1996, IEEE Electron. Device. Lett., vol. 17, pp. 473-475.
- 13 B. Georgescu, M. A. Py, A. Souifi, G. Post, and G. Guillot, "New aspects and Mechanism of kink effect in InAlAs/InGaAs/InP inverted HFET's," 1996, IEEE Electron. Device. Lett., vol. 19, pp. 154-156.

## FIGURES CAPTION

Fig. 1. Schematic cross section of MM-HEMTs structure on GaAs substrate.

Fig. 2. EL spectrum of the 0.3 MM-HEMT for  $V_{DS} = 3$  V and  $V_{GS} = -0.4$  V and of the 0.5 MM-HEMT for  $V_{DS} = 2$  V and  $V_{GS} = -0.4$  V ( $L_G = 0.1 \mu\text{m}$ ).

Fig. 3. I-V characteristics of the 0.5 MM-HEMT for  $L_G = 0.1 \mu\text{m}$  in dark (+) and under illumination ( $\bullet$ ).  $V_{GS}$  varied from 0 V to  $-1.2$  V by steps of  $-0.1$  V. The corresponding electroluminescence threshold are represented. The onset of the kink strongly coincides with the electroluminescence threshold.

Table. 1. The measured electroluminescence threshold  $V_{TH}$  for different gate lengths and Indium contents, and the corrected value  $V_{EL-T}$  after subtracting the measured voltage drop in the device access resistances.  $V_{EL-T}$  at  $x=0.5$  particularly for  $L_G = 0.1 \mu\text{m}$  is smaller than  $1.1x E_G$ , an accepted value for energy threshold of impact ionization.

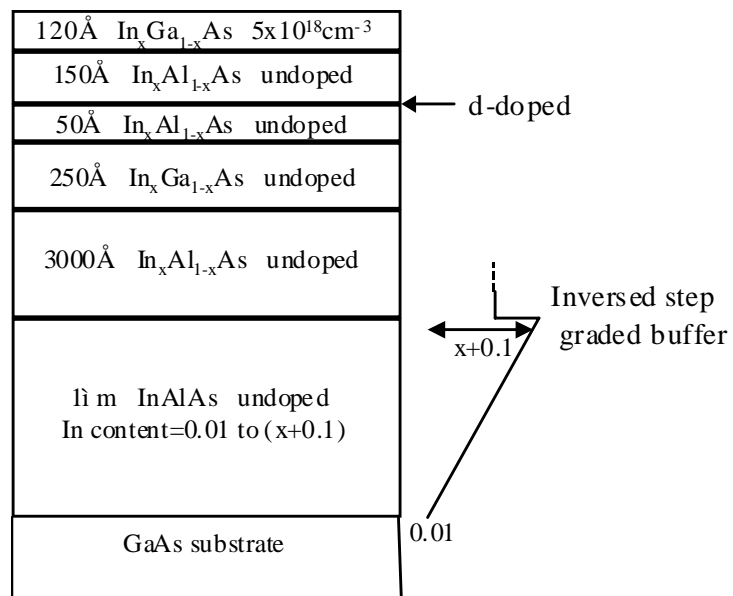


Fig. 1

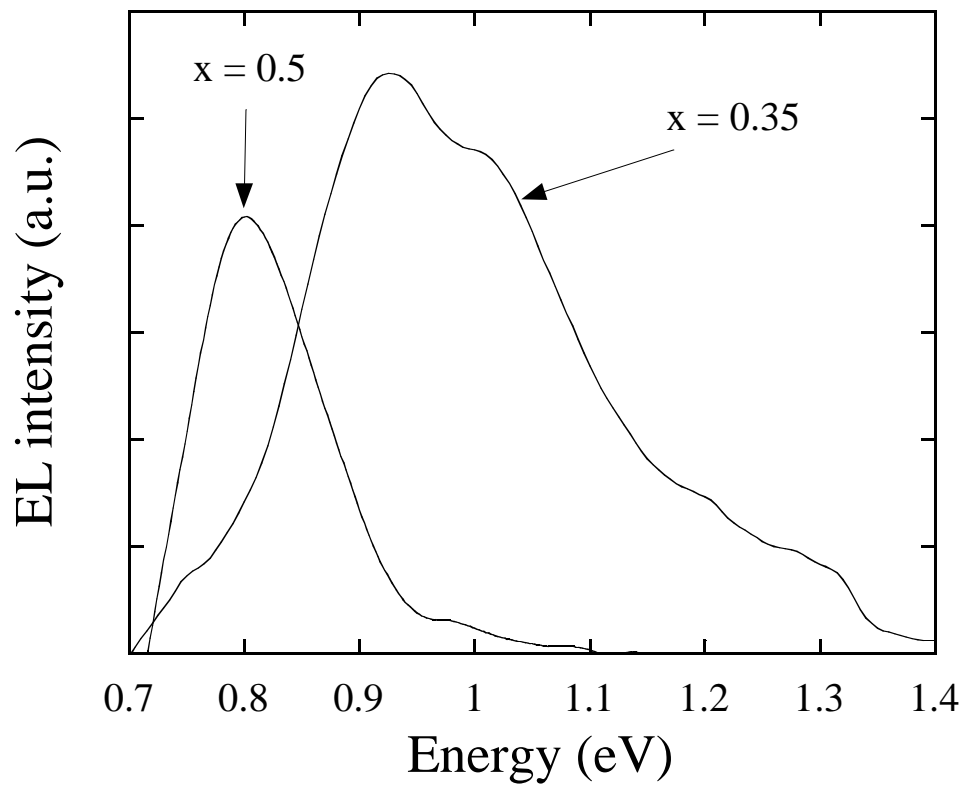


Fig. 2



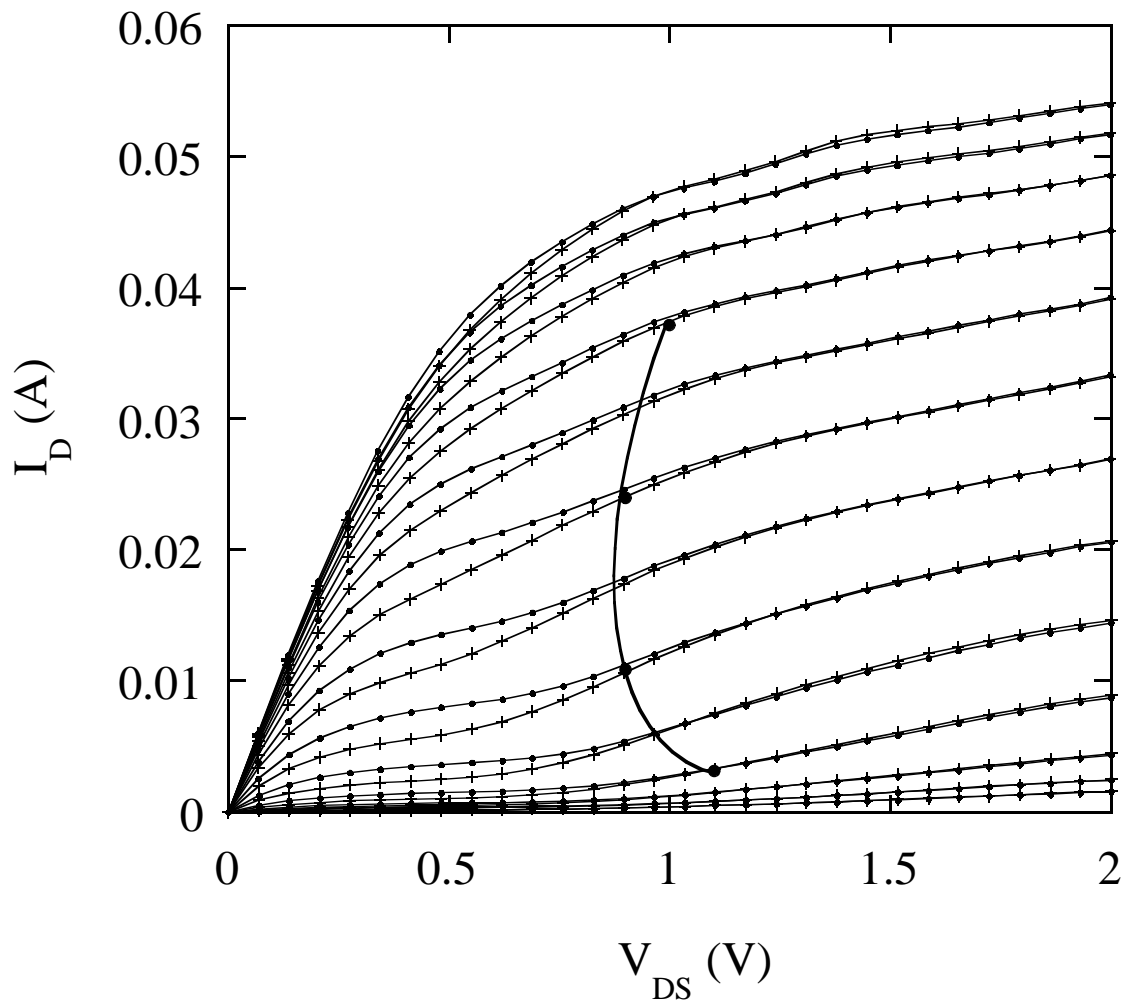


Fig. 3 (a)

In Content (%)	$L_G$ ( $\mu\text{m}$ )	$R_S$ ( $\bullet$ )	$R_D$ ( $\bullet$ )	$I_{DS}$ (mA)	$V_{TH}$ (V) measured	$V_{EL-T}$ (V) corrected	$1.1x E_G$ (eV)
50	0.1	2.3	6.95	34	0.9	0.58	0.88
50	0.15	2.3	6.9	21	1.05	0.86	0.88
35	0.1	1.3	4.75	60	1.5	1.14	1.05
35	0.15	1.3	4.8	58	1.6	1.25	1.05

Table. 1